Hydrogen evolution during deposition of microcrystalline silicon by chemical transport

Journal:	*Philosophical Magazine & Philosophical Magazine Letters*
Manuscript ID:	TPHM-07-Jul-0204.R1
Journal Selection:	Philosophical Magazine
Date Submitted by the Author:	19-Oct-2007
Complete List of Authors:	HADJADJ, Aomar; Unité de Thermique et Analyse Physique EA 3802, Faculté des Sciences, Université de Reims PHAM, Nans; UTAP - LPICM Roca i Cabarrocas, Pere; LPICM Beorchia, Adrien; UTAP Kail, Fatiha; LPC2ME
Keywords:	amorphous silicon, diffusion, hydrogenation, microcrystalline silicon, plasma processing
Keywords (user supplied):	amorphous silicon, diffusion, hydrogenation

Hydrogen evolution during deposition of microcrystalline silicon by chemical transport

N. PHAM †‡, P. ROCA i CABARROCAS ‡, A. HADJADJ*†, A. BEORCHIA† and F. KAIL§

†Laboratoires d'Analyse des Solides, Surfaces et Interfaces, Unité de Thermique et Analyse Physique, Université de Reims BP 1039, 51687 Reims, France.

‡Laboratoire de Physique des Interfaces et Couches Minces
Ecole Polytechnique, 91128 Palaiseau, France.

§Laboratoire de Physique des Couches Minces et Matériaux pour l'Electronique,
Faculté des Sciences, Université d'Oran-Es-Sénia, Algérie.
*Corresponding author. E-mail: aomar.hadjadj@univ-reims.fr

Abstract

We have exposed a freshly deposited boron-doped hydrogenated amorphous silicon (a-Si:H) layer to a hydrogen plasma under conditions of chemical transport. *In situ* spectroscopic ellipsometry measurements revealed that atomic hydrogen impinging on the film surface behaves differently before and after crystallization. First, the plasma exposure increases the hydrogen solubility in the a-Si:H network leading to the formation of a hydrogen–rich subsurface layer. Then, once the crystallization process engages, the exceeding hydrogen starts to leave the sample. We have attributed this unusual evolution of the exceeding hydrogen to the role of the grown hydrogenated microcrystalline (μc-Si:H) layer that gradually prevents the atomic hydrogen coming from the plasma to reach the μc-Si:H/a-Si:H interface. Consequently, the hydrogen solubility, initially increased by the hydrogen plasma, recovers its initial value of an untreated a-Si:H material. To support the idea that the out-diffusion is a consequence and not the cause of the growth of the μc-Si:H layer, we have solved the combined diffusion and trapping equations that govern the hydrogen diffused into the sample,

using appropriate approximations and a specific boundary condition traducing the lack of hydrogen injection during the μc-Si:H layer growth.

Keywords: hydrogen diffusion; amorphous silicon; microcrystalline silicon; hydrogen solubility.

1 Introduction

It is well-known that hydrogen diffusion is a crucial step in film growth by chemical vapour deposition of hydrogenated amorphous silicon (a-Si:H) thin films. The interaction of atomic hydrogen with a-S:H films has been widely investigated in order to understand the kinetics of H incorporation in the film [1]. The hydrogen injection is performed either from a solid source (a deuterated a-Si:H layer) or from a gas-phase source (a H- or D-plasma or heated filament). The long range motion of hydrogen is also often evoked in the light-induced metastability in a-Si:H [2]. A better understanding of H interaction with a-Si:H will facilitate the growth of a-Si:H related materials and devices with improved electronic properties and stability.

The solid phase transformation of a-Si:H to hydrogenated microcrystalline silicon (µc-Si:H) in low temperature plasma conditions has been the subject of a large number of studies [3–10]. All the growth models of µc-Si:H agree on the fact that hydrogen is an essential ingredient in the plasma enhanced chemical vapour deposition (PECVD) of such a material [3, 11–15]. However, its exact role is still subject of broad controversies. The reasons preventing the extraction of an unambiguous relationship between the crystallites formation and the hydrogen evolution are related to the complexity of the overall PECVD process: growth via different Si precursors, hydrogen etching of weak Si–Si bonds, exothermic surface reactions of hydrogen, …

In previous studies [16, 17], we have shown that when an a-Si:H thin film is exposed to a hydrogen plasma, two processes can occur. When the walls of the reactor are clean, the hydrogen plasma leads to the etching of the a-Si:H film deposited on the heated substrate and the formation of a H–rich subsurface layer. On contrary, if the walls were previously coated with a-Si:H, the H plasma leads to the deposition of µc-Si:H by chemical transport [18, 19]. In this last case, silicon is etched from the reactor walls by

hydrogen and deposited on the heated substrate, leading to the formation of a µc-Si:H film. With the beginning of the microcrystalline layer deposition, both the thickness and H excess in the subsurface layer decrease. The hydrogen out-diffusion, inconsistent with a normal diffusion process, continues until the H–rich subsurface layer completely disappears. Although this phenomenon is, without any doubt, intimately linked to the amorphous → microcrystalline phase-transformation of the a-Si:H network, the mechanism of such a relationship remains unsolved. The purpose of this article is to prove that the out-diffusion of hydrogen can be explained thanks to the role of the grown µc-Si:H layer that gradually reduces the hydrogen supply from the plasma and then decreases the solubility of H in Si until it recovers the value of an untreated a-Si:H.

2 Experimental

Boron-doped a-Si:H is deposited in a conventional 13,56 MHz radio frequency (rf) PECVD system on 1737 a Corning glass substrate. The deposition conditions were: 71 mTorr of pure silane, 3W of rf power and a substrate temperature of 230 °C. The p-doping was obtained by adding to silane 5 mTorr of trimethylboron diluted at 2 % in hydrogen. After deposition, the film is immediately exposed to the hydrogen plasma to avoid any oxidation. Indeed a thin native oxide layer can act as an efficient barrier against the hydrogen diffusion [20]. The H plasma treatment conditions were: 1 Torr of H_2 and 30 W of rf power.

At regular intervals of time, the H plasma is stopped and an ellipsometry spectrum is recorded to check the induced changes in the film structure. *In situ* UV–visible spectroscopic ellipsometry (SE) measurements were performed within the 1.5 eV – 5 eV photon energy range. The experimental ellipsometry angles Ψ and Δ are converted

Deleted: films were

Deleted: s

Deleted: s

Deleted: were

Deleted: The

Deleted: ,

Deleted: induced by the H plasma exposure, were monitored by *in*

Deleted: 1,5

to the pseudo-dielectric function < ε > using the equation for a single interface. The pseudo-dielectric function reduces to the dielectric function ε when the reflecting sample has an infinite thickness and a smooth surface [21]. More quantitative information can be derived from the SE measurements using optical models and the Bruggeman effective medium approximation (BEMA) theory [22]. The BEMA theory is well-adapted for the interpretation of the SE measurements performed on a-Si:H and μc-Si:H materials [22, 23]**.** The dielectric function of the deposited a-Si:H is described by the Tauc-Lorentz dispersion law [24] given by:

$$\varepsilon_2(E) = \frac{A\,E_0 C\,(E-E_g)^2}{(E^2-{E_0}^2)+C^2E^2}\frac{1}{E}$$
$$\varepsilon_1(E) = \varepsilon_1(\infty) + \frac{2}{\pi}\,\Pi\int_{E_g}^{\infty}\frac{\varepsilon_2(u)}{u^2-E^2}\,du \qquad \textbf{(1)}$$

where E_0 and $\varepsilon_1(\infty)$ are respectively the resonance energy of the Lorentz oscillator and the real part of the dielectric function at high photon energies. E_g is an optical band gap useful to compare the optical properties of different samples. It is lower than the usual Tauc gap [25]. Π stands for the Cauchy principal part of the integral.

The μc-Si:H material is described by a 3-phase system: microcrystallites (reference data measured by Jellison *et al.* [26]), amorphous silicon (dispersion law of Eq. (1)) and void. To determine the amount of Si–Si bonds converted to an excess Si–H bonds (i.e. an excess of the hydrogen content) by the H plasma treatment, we have followed the approach of Mui and Smith who assumed that the basic polarizable units are Si–$Si_{4-n}H_n$ tetrahedron [27]. The evolution of the volume fraction f_H of the Si–Si_3H tetrahedron follows that of the hydrogen excess in the film [28]. The effective dielectric function of

the subsurface layer affected by the H plasma is calculated using a mixture of the same dielectric function as the bulk (Eq. (1)) plus an excess of hydrogen.

3 Results and discussion

3.1 Spectroscopic ellipsometry results

Ellipsometry is a powerful tool to study *in situ* the kinetics of the H induced modifications. Fig. 1 shows the evolution of the imaginary part of the pseudo-dielectric function $< \varepsilon_2 >$ of a p-type a-Si:H film, at various stages of its exposure to a H plasma, in the case where the reactor walls are coated with a-Si:H. The as-deposited film presents a $< \varepsilon_2 >$ spectrum characteristic of hydrogenated amorphous silicon with a broad peak around 3.6 eV. For hydrogen plasma exposure times such as $t < 7$ min (Fig. 1a), a slight shift of interference fringes towards high energies indicates a decrease in the film thickness due to the etching process. Moreover, the H in-diffusion leads to a gradual decrease of the $< \varepsilon_2 >$ peak amplitude along with a slight shift towards high energies. At 10 minutes the amplitude of $< \varepsilon_2 >$ reaches its lowest value, corresponding to the formation of a porous layer on the film surface where nucleation of crystallites can take place. Beyond a hydrogen plasma exposure duration of 15 min (Fig. 1b), the $< \varepsilon_2 >$ spectrum becomes that of a microcrystalline silicon, characterized by the appearance of a broad shoulder at 4.2 eV. The growth of the µc-Si:H layer gives rise to a shift of the interference fringes to low energy synonymous with an increase in the film thickness. At the same time, the increase in the $< \varepsilon_2 >$ peak amplitude reveals a continuous change and rearrangement in the deposited µc-Si:H layer structure making it more compact.

Deleted: during
Deleted: an
Deleted: 3,6
Deleted: H
Deleted: 7
Deleted: 4,2
Deleted: An

In order to confirm the microcrystalline character of the grown layer, we have deposited a 190 nm-thick a-Si:H film on a GaAs substrate and exposed it to a H plasma during 45 minutes. The cross-sectional transmission electron microscopy (TEM) image of Fig. 2 clearly shows the formation of a 65 nm-thick μc-S:H layer. The electron diffraction pattern corresponding to the grown layer (inset of Fig. 2) is that of a μc-Si:H structure.

Deleted: patern

Fig. 3 shows the multilayer optical model used to fit the SE spectra of Fig. 1. The model was supported by other *ex situ* characterization techniques [17–19, 28]. The surface and subsurface modifications, due to atomic H impinging on the film and diffusing through it, lead to the formation of a H–rich subsurface layer accompanied with the etching of the film surface. These effects start at the ignition of the hydrogen plasma. The etching rate as well as the time needed for the complete formation of the H–rich subsurface layer (from a few seconds to a few minutes) depends on the hydrogen plasma conditions, the substrate temperature and the film doping [17–19]. With the beginning of the microcrystalline layer deposition, both the thickness and the H excess in the subsurface layer decrease indicating the out-diffusion of hydrogen from the sample. At the steady state, the excess of the Si–Si_3H tetrahedron units in this subsurface layer (f_H) can reach 20 – 30 % [17, 18]. In the case of boron-doped a-Si:H films, it amounts to say that the hydrogen content in the subsurface layer increases from 16 at. %, in the as-deposited state, to 19 – 21 at. % after the H-plasma treatment.

We have reported in Fig. 4 the changes, versus the H plasma treatment time (t), of the thickness (d_{Total}) of the whole treated film together with that (d_{Bulk}) of the bulk a-Si:H layer (Fig. 4a), the thickness (d_H) and the H-excess volume fraction (f_H) of the H–rich subsurface layer (Fig. 4b) as well as the thickness (d_{Cryst}) and the volume fraction of crystalline phase (f_{Cryst}) of the deposited μc-Si:H layer (Fig. 4c). Fig. 4a shows that the hydrogen diffusion into the film leads, on the one hand, to the formation of the H–rich

subsurface at the expense of the a-Si:H bulk layer and, on the other hand, to the etching of the film. The etching process, with a rate of 1 nm/min, lasts the first 5 – 6 minutes of plasma treatment. The two parameters that characterize the H–rich subsurface layer (Fig. 4b) show a 3-step evolution: i) a sharp increase during the first 1 – 2 minutes, ii) a plateau that goes on until t = 9 – 10 minutes and iii) a complete disappearance after 1 – 2 minutes. The two first steps include the etching phase [8] as well as the beginning of the µc-Si:H layer deposition by chemical transport [9, 10]. The last step occurs once a ~ 25 nm-thick µc-Si:H layer is deposited with a crystalline fraction of 20 – 30 %. The hydrogen out-diffusion is also obvious through the 20 nm increase in the bulk a-Si:H layer (Fig. 4a). The results displayed in Fig. 4 allow us to draw the following conclusions: i): The µc-Si:H layer is made from silicon growth precursors coming from the plasma phase. It does not result, from a solid phase transformation of the initial a–Si:H layer but only from the top part of it. ii) The nucleation of crystallites occurs within a ~ 10 nm-thick region below the surface. iii): The out-diffusion of hydrogen from the H–rich subsurface layer accompanies the deposition of the µc-Si:H layer.

Deleted: Si

Deleted: at least not predominantly,

Deleted: H–rich subsurface

Deleted: buried

Deleted: 5

The need for an incubation (or a transition) layer for the µc-Si:H growth from an a-Si:H layer has been demonstrated by several experimental studies [4, 5, 8, 9, 29]. The transition layer was first interpreted as a porous a-Si:H layer [4, 5, 29]. Later, it was identified as a hydrogen saturated layer [16, 30]. In conditions of the solid phase transformation of a-Si:H to µc-Si:H (chemical annealing or high hydrogen chemical potential), the formation of the µc-Si:H film is often attributed to the out-diffusion of hydrogen by forming molecular hydrogen [8]. The energy released from the formation of hydrogen molecules may enhance the relaxation of Si atoms in order to form crystallites. Consequently, the crystallization results from the out-diffusion of hydrogen. Our experimental results (Fig. 4) lead to the conclusion that the out-diffusion of

hydrogen is a consequence and not the cause of the growth of the μc-Si:H layer. The trap-limited hydrogen diffusion model that we shall develop in the next section aims to prove that the grown μc-Si:H layer, gradually stops the atomic hydrogen supplied by the plasma and then induces the observed out-diffusion of hydrogen.

3.2 Hydrogen capture and release model

Our model is based on the same principle that governs the dissolution of a gas in a liquid. It is well-known that gases increase in solubility with an increase in pressure. Indeed, Henry's law [31] states that the solubility of a gas in a liquid is directly proportional to the pressure of the gas above the surface of the solution. Carbonated beverages provide the best example of this phenomenon. The carbonated beverage is bottled under pressure to increase the carbon dioxide dissolved in solution. When the bottle is opened, the pressure above the solution decreases, and as a result, the solution effervesces and some of the carbon dioxide bubbles off. An other example is given by deep sea diving. When the diver rises from the depths too fast, the nitrogen gas dissolved in the blood will come out of solution as the pressure is released and form bubbles in the blood and other body fluids.

If we consider that H atoms will behave towards the a-Si:H film in the same way of a gas with a liquid, we shall take advantage of such a phenomenon to interpret the time-dependence of the H–rich subsurface layer of Fig. 4b. In other words, in presence of the H plasma, the chemical potential of hydrogen rises leading to the H in-diffusion and trapping within the a-Si:H film. The growth of the μc-Si:H will consume most of H impinging atoms and then will reduce the amount of hydrogen reaching the μc-Si:H/a-Si:H interface. The gradual decrease in the mobile H amount will, consequently, make

the hydrogen chemical potential in the a-Si:H film. Then, the exceeding hydrogen will vanish.

Deleted: Consequently,
Deleted: will drop by the gradual decrease of the amount of mobile H
Deleted: and

We shall treat the formation of the H–rich subsurface layer within a one-dimensional diffusion of hydrogen into a semi-infinite material ($x \geq 0$). The mobile hydrogen ($C_m(x, t)$) can be captured with a rate α_τ and released with a rate α_r at hydrogen traps. We shall call N_τ the concentration of those available traps. The a-Si:H film surface is fixed at the coordinate $x = 0$ and the substrate extends to $x = \infty$. The coordinate $x = 0$ will refer to the μc-Si:H/a-Si:H interface once the deposition process of the μc-Si:H layer by chemical transport starts. If we neglect the shift of the film surface during the etching process, the concentration of hydrogen diffusing into the sample and that of hydrogen trapped ($C_\tau(x, t)$) are governed by the following set of equations:

$$\frac{\partial C_m(x,t)}{\partial t} = D_H \frac{\partial^2 C_m(x,t)}{\partial x^2} - \frac{\partial C_\tau(x,t)}{\partial t} \quad \textbf{(2)}$$

$$\frac{\partial C_\tau(x,t)}{\partial t} = \alpha_\tau \left[1 - \frac{C_m(0)}{N_\tau} C_\tau(x,t)\right] C_m(x,t) - \alpha_r C_\tau(x,t) \quad \textbf{(3)}$$

The capture rate α_τ can be linked to the density of traps N_τ and their capture radius R_τ by [32]:

$$\alpha_\tau = 4\pi R_\tau D_H N_\tau \quad \textbf{(4)}$$

The following points concerning the diffusion model must be emphasized:

(i) The model only aims to interpret the evolution of the subsurface layer during the H plasma treatment. It does not deal with the deposition process of the microcrystalline layer.

(ii) All H atoms involved in Eqs. (2) and (3) are additional H atoms incorporated in the a-Si:H film during the H plasma treatment. The initial tightly bonded H atoms are not concerned.

(iii) Although high values ($> 10^{-10}$ cm^2s^{-1}) of the hydrogen diffusivity D_H at the very initial stage of hydrogen plasma treatment have been reported by several authors [20, 33-35], we assume that, during all the plasma treatment, the transport of atomic H is characterized by a constant D_H. Moreover, a quite important concentration-dependence of D_H has also been reported [36].

(iv) We have considered only one trapping level and a uniform and constant density of traps N_τ. We shall not make any allusion to the microscopic nature of the trapping sites. In this way, contrary to some H diffusion models in p-type a-Si:H [37], we shall not differentiate the dopant atoms, that can trap hydrogen, from other types of hydrogen traps.

(v) Eqs. (2) and (3) do not refer to the charge state of the diffusing H even if some recent reported results indicate that H is very likely to be positively charged in the p–type a–Si:H [38–41]. An electric field effect (due, for example, to the local electric field that could arise at the μc-Si:H/a-Si:H heterojunction) cannot be excluded [42].

(vi) As we did in a previous paper [17], we shall associate the hydrogen excess in the subsurface layer determined by SE measurements with the concentration of trapped hydrogen $C_t(x, t)$. Indeed, a non-bonded H does not give a significant contribution to the dielectric function of the film [20].

3.2.1 Kinetics of hydrogen trapping. Fig. 4b suggests that the formation of the H–rich subsurface layer corresponds to the phase where the trapping process is predominant. If we neglect the reemission process, Eq. (3) can be easily integrated leading to the following expression of $C_\tau(x, t)$:

$$C_\tau(x,t) = N_\tau\left[1 - exp\left(-\frac{\alpha_\tau}{N_\tau}\int_0^t C_m(x,t')\,\mathrm{d}t'\right)\right] \quad \textbf{(5)}$$

To find an analytical solution $C_m(x, t)$ of Eq. (2), one has to drop the coupled term. This simplification amounts to underestimate the trapping rate α_τ. At the beginning of the H plasma exposure, the initial conditions for the set of equations (2) and (3) are: $C_m(x, 0) = C_m(0)$ for $x \leq 0$, $C_m(x, 0) = 0$ for $x > 0$ and $C_\tau(x, 0) = 0$. As the sample thickness always remains larger than the hydrogen diffusion length, one boundary condition is to consider that $C_m(\infty, t) = 0$ and $C_\tau(\infty, t) = 0$ for $t \geq 0$. The rapid formation of the H– rich subsurface layer (almost one minute) suggests a high value for the time factor in the exponential term of Eq. (5). If we call $C_m(0)$ the concentration of mobile H at the film surface, large values are expected for the ratio $C_m(0)/N_\tau$. In fact, in the case of "normal" or unattenuated H plasma, the flux of atomic hydrogen at the film surface is around 10^{14} $cm^{-2}s^{-1}$ [43]. With an etching rate of 1 nm/min a value of $C_m(0) > 10^{21}$ cm^{-3} is expected. Moreover, values as high as $10^{20} – 10^{21}$ cm^{-3} were experimentally measured for the H surface concentration [36, 44–47].

Since the formation of microcrystalline nucleus, H atoms coming from the plasma will rather be involved in the growth of the crystalline grains and, consequently, will not reach the µcSi:H/a-Si:H interface. Consequently, the deposition of the µcSi:H layer

Deleted: estimated

Deleted: en

from growth precursors [48] may explain the observed out-diffusion of hydrogen. Many researchers have reported the transformation of a-Si:H to μc-Si:H with a concomitant out-diffusion of hydrogen. Using *in situ* SE and infrared attenuated total reflection spectroscopy measurements, Fujiwara *et al.* studied the initial layers from which μc-Si:H nucleates, in a rf PECVD process, with increasing the $[H_2]/[SiH_4]$ dilution [49]. These authors showed that the μc-Si:H formation reduces the incorporation of Si–H and $Si–H_2$ bonds in the a-Si:H bulk layer. Katiyar and Abelson have exposed a freshly deposited a-Si:H film to H plasma [9]. They observed a decrease in the 2000 cm^{-1} infrared mode which accompanies the formation of μc-Si:H on the a-Si:H film.

Thus, once the μc-Si:H layer starts to grow at $t = T_1 = 5$ min (Fig. 4c), less and less hydrogen atoms reach the μcSi:H/a-Si:H interface. As a result, the H chemical potential, initially raised by the H plasma, will decrease during the growth of the μc-Si:H layer. To express the fact that, after a time θ, hydrogen atoms cannot any more reach the μcSi:H/a-Si:H interface, we can use the following boundary condition:

Formatted: Font: Symbol

Deleted: This effect can be expressed by

Deleted: at the film surface ($x = 0$)

$$C_m(0,t) = \begin{cases} C_m(0) & t \le T_1 \\ C_m(0)\exp\left(-\dfrac{t-T_1}{\theta}\right) & t > T_1 \end{cases} \quad \textbf{(6)}$$

With the mentioned initial and boundary conditions, an exact analytical solution of Eq. (2) can be found:

$$C_m(x,t) = \begin{cases} C_m(0)\,\mathrm{f}(x,t,\infty) & t \le T_1 \\ C_m(0)\left(\mathrm{f}(x,t,\infty) + \mathrm{f}(x,t-T_1,\theta) - \mathrm{f}(x,t-T_1,\infty)\right) & t > T_1 \end{cases} \quad \textbf{(7)}$$

where the function $f(x, t, \theta)$ is defined by:

$$f(x,t,\theta)=\frac{1}{2}\exp\left(-\frac{t}{\theta}\right)\left[\exp\left(x\sqrt{\frac{\alpha_\tau-\frac{1}{\theta}}{D_H}}\right)\operatorname{erfc}\left(\frac{x}{2\sqrt{D_H t}}+\sqrt{\left(\alpha_\tau-\frac{1}{\theta}\right)t}\right)\right.$$
$$\left.+\exp\left(-x\sqrt{\frac{\alpha_\tau-\frac{1}{\theta}}{D_H}}\right)\operatorname{erfc}\left(\frac{x}{2\sqrt{D_H t}}-\sqrt{\left(\alpha_\tau-\frac{1}{\theta}\right)t}\right)\right] \quad \textbf{(8)}$$

The exponential behaviour of $C_\tau(x)$ profile tail (see Fig. 5), allows us to define an effective diffusion length L_D by:

$$\frac{C_\tau(L_D,t)}{C_\tau(0,t)}=\frac{1}{e} \quad \textbf{(9)}$$

If we identify the mean diffusion length L_D with the thickness d_H of the H–rich subsurface layer, we shall be able to determine both the diffusion coefficient D_H and the capture rate α_τ (and consequently the density of traps N_τ). Indeed, one can determine these two parameters (D_H and α_τ) by minimizing the following quantity:

$$\sum_j\left[C_\tau(d_H,t)-\frac{1}{e}\right]^2 \quad \textbf{(10)}$$

The summation j is over the (t, d_H) experimental couples for times such as $t \leq 9$ min (before the H–rich subsurface layer starts to vanish, see Fig. 4b). Assuming $C_m(0)/N_\tau = 10$ and using $T_1 = 5$ min and $\theta = 1$ min, the fit of the experimental results leads to: $D_H = 2.09\text{x}10^{-14}$ cm^{2}s^{-1} and $\alpha_\tau = 1.35\text{x}10^{-1}$ s^{-1}. The value of D_H is consistent with those

Deleted: 2,09

Deleted: 1,35

reported in the case of diffusion from the plasma [46]. As a comparison, in the case of intrinsic a-Si:H, we have found that D_H decreases from 3.0×10^{-14} to 2.4×10^{-13} $cm^2 s^{-1}$ when the temperature of H plasma treatment is raised from 100 to 250 °C [17]. At the same time, α_τ decreases from 5.5×10^{-2} to 2.7×10^{-2} s^{-1}. An *et al.* have exposed intrinsic a-Si:H to atomic H generated by a filament heated in H_2 with a substrate temperature of 250 °C [20]. They estimated a value of ~ 10^{-3} s^{-1} for α_τ.

We do not know the capture radius for a hydrogen trapping centre R_τ. If we assume it constant and roughly equal to the size of a dangling bond $R_\tau \approx 0.2$ nm [17, 44], then we derive a density of traps $N_\tau = 2.57 \times 10^{19}$ cm^{-3}. Such a value of N_τ is two orders of magnitude higher than that determined in the case of undoped a-Si:H exposed to a H plasma at the same temperature [17]. Furthermore, N_τ is about one order of magnitude higher than the defect density (mainly isolated dangling bonds) induced by the boron doping in a-Si:H [50].

In Fig. 5 are plotted the concentration profiles $C_m(x)$ and $C_t(x)$ at different times obtained using the values of $D_H = 2.09 \times 10^{-14}$ $cm^2 s^{-1}$, $\alpha_\tau = 1.35 \times 10^{-1}$ s^{-1}, $C_m(0)/N_\tau = 10$, $T_1 = 5$ min and $\theta = 1$ min. Before the deposition of the microcrystalline layer ($t < T_1$), both C_m and C_τ rapidly extend and reach a saturation limit. We have already reported such a behaviour in H plasma conditions where only the etching of a-Si:H takes place [17]. This rapid diffusion agrees with the abrupt formation of the H–rich subsurface layer (Fig. 4b). Beyond the etching phase and during the crystallization process ($t > T_1$), the sample starts to run out of mobile hydrogen. Consequently, the H trapped profile remains unchanged.

The integrated amount of mobile (or trapped) hydrogen $Q_{m,\tau}$ within the whole film thickness can be defined by:

Deleted: 3,0
Deleted: 2,4
Deleted: 5,5
Deleted: 2,7
Deleted: 2,57
Deleted: 2,09
Deleted: 1,35

$$Q_{m,\tau}(t) = \int_0^\infty C_{m,\tau}(x,t)\,\mathrm{d}x \qquad (11)$$

Fig. 6 shows the time-dependence of the Q_m/Q_τ ratio, deduced from the hydrogen profiles of Fig. 5. Although Q_m/Q_τ gradually decreases for $t < T_1$, the amount of mobile hydrogen remains higher than that trapped in the H–rich subsurface layer. Within this range of time, the capture process of hydrogen is the prevailing one. Beyond $t = T_1$, the ratio Q_m/Q_τ undergoes a drastic fall. Such a sharp depletion in mobile hydrogen marks the end of the predominance of the hydrogen capture process. According to Figs. 4 and 6, the H–rich subsurface layer starts to vanish for plasma exposure times higher than 10 min. This when $Q_m/Q_\tau < 0{,}1$.

3.2.2 Kinetics of hydrogen release The growth of the µc-Si:H layer prevents the H atoms coming form the plasma to reach the µc-Si:H/ a-Si:H interface. Consequently, by analogy with the gas dissolution in a liquid, the H pressure above the a-Si:H surface vanishes leading to a decrease in the H solubility in the a-Si:H network.. According to Fig. 4, this process starts at $t = T_2 = 8 - 9$ min and lasts a time $\delta = 1 - 2$ min. During this period of time, the H reemission becomes predominant at the expense of the trapping process. In this case, the integration of Eq. (3) leads to:

$$Q_\tau(t) = Q_\tau(T_2)\exp\left[-\alpha_r(t - T_2)\right] \qquad t \geq T_2 \qquad (12)$$

The characteristic time δ can be identified as the inverse of the release rate α_r. Thus, a value of $\delta = 1 - 2$ min leads to $\alpha_r = 0.8 - 1.7 \times 10^{-2}$ s^{-1}. In the case of the hydrogenation

Deleted: 0,8

Deleted: 1,7

of intrinsic a-Si:H at 250 °C with a heated filament, An *et al.* have found a quite lower reemission rate ($\alpha_r < 2\text{x}10^{-7}$ s^{-1}) upon extinguishing the heated filament [20]. In Fig. 7 we compare the calculated value $Q_t(t)$ with the experimental $d_H(t)$ x $f_H(t)$ product at different H plasma exposure times. Both experimental and calculated values are normalized with respect to $t = T_2$. The calculations were performed using: D_H = $2.09\text{x}10^{-14}$ cm^2s^{-1}, $\alpha_\tau = 1.35\text{x}10^{-1}$ s^{-1}, $C_m(0)/N_\tau = 10$, $T_1 = 5$ min and $\theta = 1$ min, for the H trapping process, and α_r = $1.7\text{x}10^{-2}$ s^{-1}(δ = 1 min) and T_2 = 9 min for the H reemission process. Fig. 7 displays a good agreement between calculated and experimental results within the whole time-range.

Deleted: 2,09

Deleted: 1,35

Deleted: 1,7

We do not know exactly how the released H atoms do leave the subsurface layer. Probably hydrogen desorbs by simultaneous rupture of two Si–H bonds and forms H_2 molecules. A direct abstraction of a bonded H by a mobile atomic H, like a Eley-Rideal mechanism, cannot be excluded since such a mechanism involves a low activation barrier energy [52]. The hydrogen molecules may leave the film by rapid diffusion through voids, that could be formed by the H plasma treatment [51] in a–Si:H or grain boundaries of the μc-Si:H layer [1, 53, 54]. The low sticking coefficient of H_2 on Si at moderate temperature [55], favours the rapid out-diffusion of hydrogen. Moreover, some theoretical works point out a number of arguments that relate the possibility of molecular hydrogen playing an important role in the observed transport of hydrogen in a-Si:H [56–58]. Some works might even find H_2 more mobile than H [59]. The formation of H_2 molecules in a silicon network, after a post-hydrogenation, has been demonstrated by many experimental works. In the case of crystalline silicon, molecular hydrogen occupies the cavities induced by the hydrogenation [60]. In the case of micro- and nanocrystallized silicon films the presence of molecular hydrogen is detected in surface cavities as well as at grain boundaries [61]. Moreover, in hydrogen effusion

experiments, the low temperature (~ 400 °C) effusion peak, in a-Si:H and μc-Si:H deposited at low temperature, is often attributed to the rapid diffusion of molecular hydrogen (H_2, D_2 and HD) [1]. It is also correlated to the presence of an interconnected void network in material deposited at low temperature. The low temperature effusion process is found not to be limited by diffusion as the effusion peak temperature is independent of film thickness. Further investigations are needed to probe other tracks in order to clarify how does happen the observed out-diffusion of hydrogen.

4 Summary

We have investigated the hydrogen plasma treatment of p-type a-Si:H films in conditions of μ-Si:H deposition by chemical transport. We dealt with the kinetics of hydrogen excess evolution during the plasma exposure and particularly its out-diffusion when the crystallization of the film starts. To interpret the experimental results, we have solved the combined diffusion and trapping equations that govern the H-diffusion into the sample. We have used a specific boundary condition that accounts for the reduction of the atomic H flux with the growth of the μc-Si:H layer. The proposed model explains the experimentally observed evolution of hydrogen during the plasma treatment. Moreover, it supports the idea that the out-diffusion is a consequence and not the cause of the growth of the μc-Si:H layer.

REFERENCES

[1] W. Beyer, Sol. Energ. Mater. Sol. Cells, **78** 235 (2003).

[2] M.H. Branz, Sol. Energ. Mater. Sol. Cells, **78** 45 (2003).

[3] S. Veprek, Z. Iqbal, H. R. Ostwald and P. Webb, J. Phys. **C 14** 295 (1981).

[4] N. Layadi, P. Roca i Cabarroca, B. Drévillon and I. Solomon, Phys. Rev. **B 52** 5136 (1995).

[5] P. Roca i Cabarroca, N. Layadi, B. Drévillon and I. Solomon, J. Non-Cryst. Solids **198-200** 871 (1996).

[6] S. Hamma and P. Roca i Cabarrocas, J. Appl. Phys. **81** 7282 (1997).

[7] A. Matsuda, Thin Solid Films **337** 1 (1999).

[8] J. Jang. S.O. Koh, T.G. Kim and S.C. Kim, Appl. Phys. Lett. **60** 2874 (1992).

[9] M. Katiyar and J. R. Abelson, Mat. Sci. Eng. **A 304-306** 349 (2001).

[10] B. Lyka, E. Amanatides and D. Mataras, J. Non-Cryst. Solids **352** 1049 (2006).

[11] I. Solomon, B. Drévillon, H. Shirai and N. Layadi, J. Non-Cryst. Solids **164** 989 (1993).

[12] A. Matsuda and K. Tanaka, J. Non-Cryst. Solids **114** 1367 (1987).

[13] H. Shirai, D. Das, J. Hamma and I. Shimizu, Appl. Phys. Lett. **59** 1096 (1991).

[14] M. Otobe, and S. Oda, J. Non-Cryst. Solids **164** 993 (1993).

[15] R.A. Street, Phys. Rev. **B 43** 2454 (1991).

[16] A. Fontcuberta i Morral, and P. Roca i Cabarrocas, J. Non-Cryst. Solids **299-302** 196 (2002).

[17] F. Kail, A. Fonctcuberta i Morral, A. Hadjadj, P. Roca i Cabarrocas and A. Beorchia, Philos. Mag. **21** 595 (2004).

[18] F. Kail, A. Hadjadj and .P. Roca i Cabarrocas, Proceedings of 19th European photovoltaic Solar Energy Conference, Paris, June 7-11 (2004) FRANCE, Eds. W. Hoffmann, J.-L. Bal , H. Ossenbrink, W. Palz and P. Helm, p. 1367.

[19] F. Kail, A. Hadjadj and P. Roca i Cabarrocas, Thin Solid Films **126-131** 487 (2005).

[20] I. An, Y.M. Li, C.R. Wronski and R.W. Collins, Phys. Rev. **B 38** 4464 (1993).

[21] R.M. Azzam and N.M. Bashara, in *Ellipsometry and Polarized Light*, North-Holland, Amsterdam (1997), p. 274.

[22] D.E. Aspnes, Thin Solid Films **89** 249 (1982).

[23] P. Roca i Cabarrocas, S. Hamma and A. Hadjadj, Appl. Phys. Lett. **69** 1 (1996).

[24] G.E. Jellison and Jr and F.A. Modine, Appl. Phys. Lett. **69** 371 (1996).

[25] J. Tauc and A. Menth, J. Non-Cryst. Solids **8-10** 569 (1972).

[26] G.E. Jellison, Jr M.F. Chisholm and S.M. Gorbatkin, Appl. Phys. Lett. **62** 3348 (1993).

[27] K. Mui and F. Smith, Phys. Rev. **B 38** 10623 (1988).

[28] A. Fontcuberta i Morral and P. Roca i Cabarrocas, Phys. Rev. **B 69** 125307-1 (2004).

[29] S. Hamma and P. Roca i Cabarrocas, J. Appl. Phys. **81** 7282 (1997).

[30] A. von Keudell and J.R. Robertson J. Appl. Phys. **84** 489 (1998).

[31] P.W. Atkins in *General Chemistry*, Ed W.H. Freeman and Company, Scientific American Books, New York and Oxford (1992).

[32] T.R. Waite, Phys. Rev. **107** 463 (1957).

[33] U.K. Das, T. Yasuda and S. Yamasaki, Phys. Rev. Lett. **85** 2324 (2000).

[34] U. K. Das, T. Yasuda and S. Yamasaki, Phys. Rev. **B 63** 245204 (2001).

[35] S. Yamasaki, U.K. Das and T. Yasuda, J. Non-Cryst. Solids **299-302** 185 (2002).

[36] N.H. Nickel, W.B. Jackson and J. Walker, Phys. Rev. **B 53** 7750 (1996).

[37] A. Saad, O.I. Velichko, Y.P. Shaman, A.V. Mazanik, A.K. Fedotov and V.V. Fedotova, Nuc. Instrum. Meth. Phys. Res. **B 253** 118 (2007).

[38] H.M. Branz, R. Reedy, R.S. Crandall, H. Mahan, Y. Xu and B.P. Nelson, J. Non-Cryst. Solids **299-302** 191 (2002).

[39] W. Beyer in *Semiconductors and Semimetals*, Edits. R.K. Wielardson and E.R. Weber, Academic Press, San Diego 1999, Vol 61.

[40] P.A. Fedders, Phys. Rev. **B 66** 195308-1 (2002).

[41] N.M. Johnson and C. Herring, Phys. Rev. **B 38** 1581 (1988).

[42] A. Fontoni, M. Vieira and R. Martins, Thin Sold Flms **337** 109 (1999).

[43] T. Novikova, B. Kalache, P. Bulkin, K. Hassouni, W. Morscheidt and P. Roca I Cabarrocas, J. Appl. Phys. **93** 3198 (2003).

[44] W.B. Jackson and C.C. Tsai, Phys. Rev. **B 45** 6564 (1992).

[45] N.H. Nickel and I.E. Beckers, Phys. Rev. **B 66** 075211-1 (2002).

[46] P.V. Santos and W.B. Jackson, Phys. Rev. **B 46** 4595 (1992).

[47] S. Darwiche, M. Nikravech, D. Morvan, J. Amouroux and D. Balllutaud, Sol. Energ. Mater. Sol. Cells **91** 195 (2007).

[48] S. Veprek, Z. Iqbal and F.A. Sarott, Phil. Mag. **B 45** 137 (1982).

[49] H. Fujiwara, Y. Toyoshima, M. Kondo and A. Matsuda, J. Non-Cryst. Solids **266-269** 38 (2000).

[50] A Hadjadj, P. St'ahel, P. Roca i Cabarrocas, V. Paret, Y. Bounouh and J. C. Martin, J. Appl. Phys. **83** 830 (1998).

[51] N.M. Johnson; F.A. Ponce; R.A. Street and R.J. Nemanich Phys. Rev. **B 35** 4166 (1987).

[52]. S. Agarwal, A. Takano, M.C.M. van de Sanden, D. Maroudas and E.S. Aydil, J. Chem. Phys. **117** 10805 (2002).

[53] D.K. Biegelsen, R.A. Street, C.C. Tsai, J.C. Knights, Phys. Rev. **B 20** 4839 (1979).

[54] W. Beyer, H. Wagner, H. Mell, Solid State Commun. **39** 375 (1981).

[55] M. Durr and U. Hofer, Surf. Sci. Reports **61** 465 (2006).

[56] P.A. Fedders, Phys. Rev. **B 61** 15797 (2000).

[57] P.A. Fedders, D.J. Leopold, P.H. Chan, R. Borzi and R.E. Norberg, Phys. Rev. Lett. **85** 401 (2000).

[58] T. Su, S. Chen, P.C. Taylor, R.S. Crandall and A.H. Mahan, Phys. Rev. **B 62** 12849 (2000).

[59] T.A. Abtew, F. Inam and D.A. Drabold, Los Alamos National Laboratory, Preprint Archive, Condensed Matter 1 (2006).

[60] Y. Ma, R. Job, Y.L. Yuang, W.R. Fahrner, M.F. Beaufort, S. Rousselet and J.T. Horstmann, Appl. Phys. Lett. **86** 252109-1 (2005).

[61] L. Lusson, P. Elkaim, A. Correia and D. Ballutaud, J. Physique **III 5** 1173 (1995).

FIGURE CAPTIONS

Figure 1: Imaginary part of the pseudo-dielectric function of the a-Si:H film thickness during the H plasma exposure, (a): before and (b): after the µc-Si:H layer deposition. The arrow indicates the position of the broad shoulder which is a signature of the µc– Si:H material.

Figure 2: Cross-section TEM of an 190 nm-thick a-Si:H film deposited on a GaAs substrate and exposed to a H plasma during 45 minutes. The treatment leads to the formation of a 65 nm-thick µc-Si:H. The inset displays the electron diffraction patern of the crystallized layer.

Figure 3: Schematic of the multilayer optical model used to fit the SE measurements of Fig. 1:
(a) : In its as-deposited state, the a-Si:H film is constituted by a bulk and a surface roughness.
(b) : From the ignition of the H plasma, a H–rich subsurface layer starts to form accompanied by an etching of the film.
(c) and (d) : When µc-Si:H deposition by chemical transport starts, an out-diffusion of hydrogen leads to the disappearance of the H–rich subsurface layer.

Figure 4: Time-evolution of (a) : the thickness of the whole film d_{Total} and the thickness of the a-Si:H bulk layer d_{Bulk}, (b) : the thickness d_H and the H-excess fraction f_H of the H–rich subsurface layer and (c) : the thickness d_{Cryst} and the crystalline volume fraction f_{Cryst} of the µc-Si:H layer deposited by chemical transport during the H plasma exposure. The curves are provided as guides for the eye. The arrows indicate the values of the etching duration T_1 and the time T_2 at which the hydrogen out-diffusion starts.

Figure 5: Concentration profiles $C_m(x, t)$ and $C_\tau(x, t)$ at different H plasma treatment times. The values used for the calculations are: $D_H = 2.09 \times 10^{-14}$ cm^{2}s^{-1}, $\alpha_\tau = 1.35 \times 10^{-1}$ s^{-1}, $C_m(0)/N_\tau = 10$, $T_1 = 5$ min and $\theta = 1$ min.

Formatted: Font: Symbol

Deleted: 2,09

Deleted: 1,35

Figure 6: Time-dependence of the ratio Q_m/Q_τ deduced from the hydrogen profiles of Fig. 5. The arrows indicate the end of the etching (T_1) and the beginning of the disappearance of the H–rich subsurface layer (T_2).

Figure 7: Experimental (d_H x f_H) and calculated (Q_τ) integrated amount of trapped hydrogen versus the time of the H plasma exposure. The values used for the calculations are: $D_H = 2.09\text{x}10^{-14}$ cm^{2}s^{-1}, $\alpha_\tau = 1.35\text{x}10^{-1}$ s^{-1}, $C_m(0)/N_\tau = 10$, $T_1 = 5$ min and $\theta = 1$ min, for the trapping process (solid curve), and $\alpha_r = 1.7\text{x}10^{-2}$ s^{-1}, $T_2 = 9$ min and $\delta = 1$ min for the reemission process (dashed curve). The data are normalized with respect to their values at $t = T_2$.

Deleted: 2,09

Deleted: 1,35

Deleted: 1,7

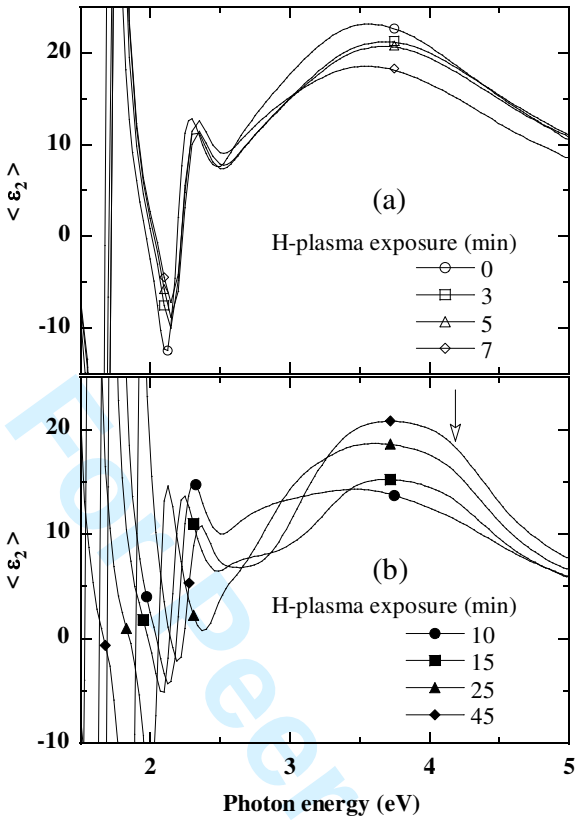

Figure 1

N. PHAM *et al.*

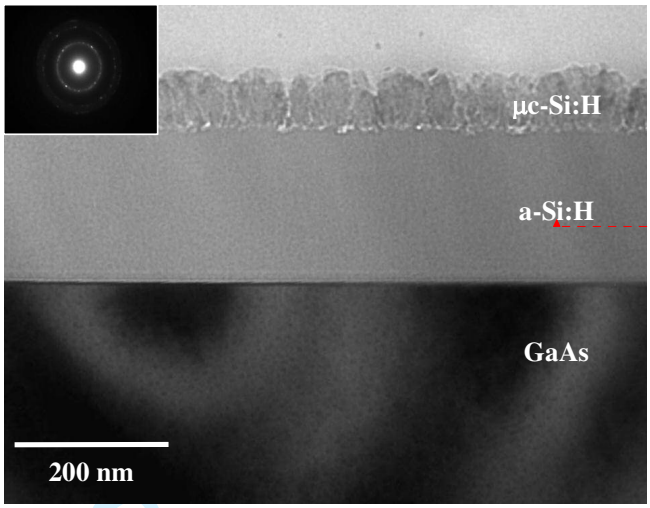

Formatted: Font: Bold, Font color: White

Figure 2

N. PHAM *et al.*

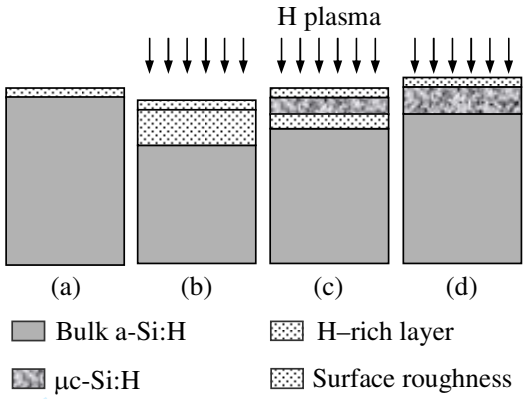

Figure 3

N. PHAM *et al.*

3

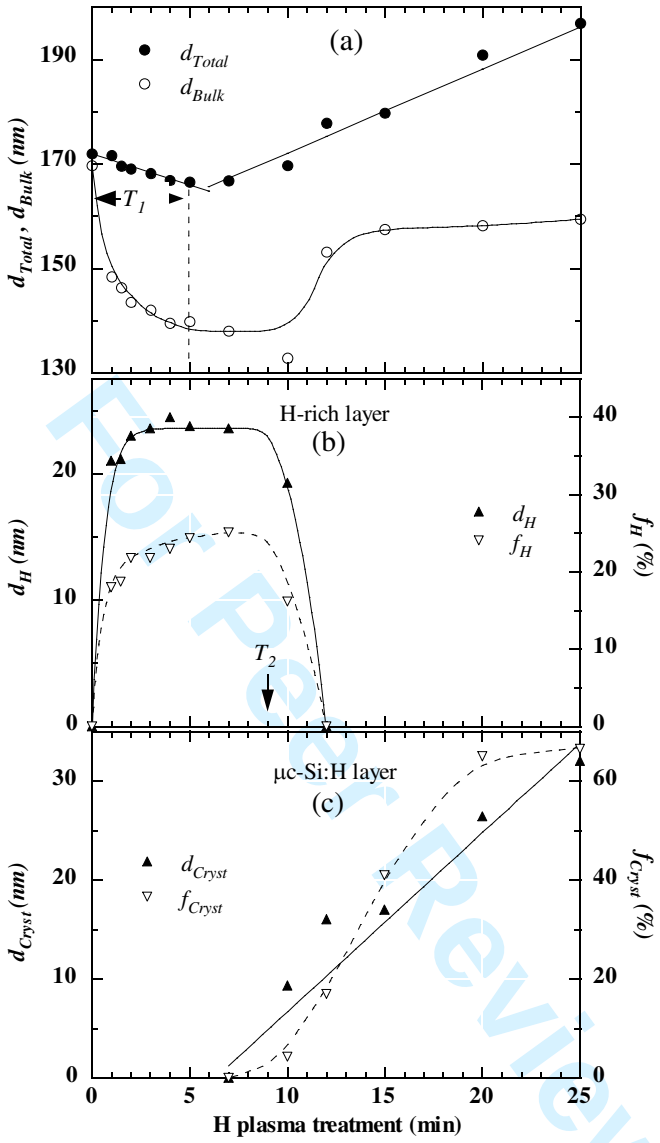

Figure 4

N. PHAM *et al.*

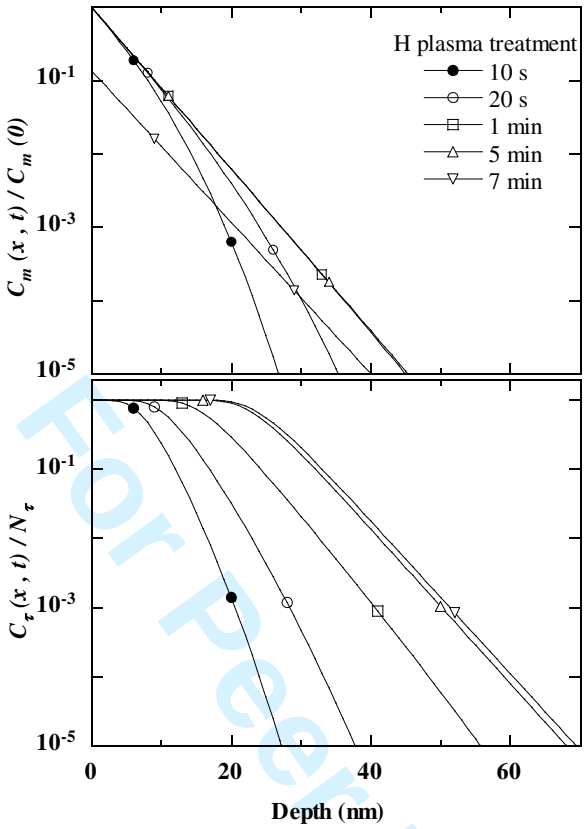

Figure 5

N. PHAM *et al.*

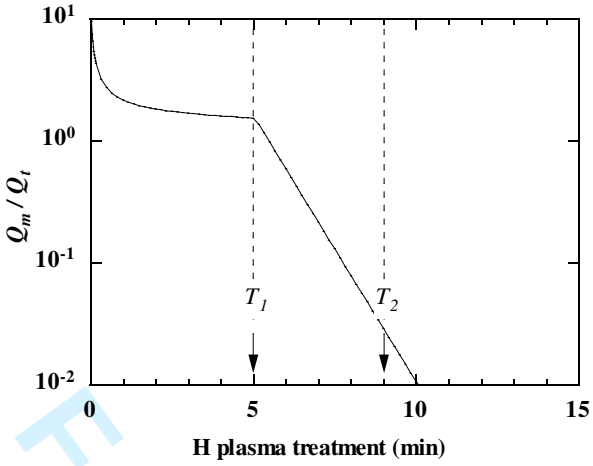

Figure 6

N. PHAM *et al.*

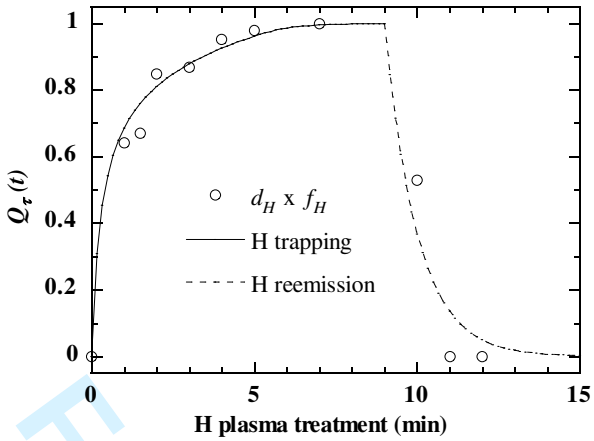

Figure 7

N. PHAM *et al.*